Journal of Sol-Gel Science and Technology (2018) 87:83–94
https://doi.org/10.1007/s10971-018-4707-x

ORIGINAL PAPER: FUNDAMENTALS OF SOL–GEL AND HYBRID MATERIALS PROCESSING

Thermal stability of Al-modified silica aerogels through epoxide-assisted sol–gel route followed by ambient pressure drying

Xuan Ling[1] · Bo Li[1,2] · Mengmeng Li[1] · Wenbin Hu[1,3] · Wei Chen[1,2]

Received: 8 February 2018 / Accepted: 19 May 2018 / Published online: 4 June 2018

Abstract

A novel method for preparing Al-modified silica aerogels with pretreated kaolin as the raw material is developed. Sols comprising silica and Al are prepared by an in situ reaction method from pretreated kaolin. The pretreatment step simplifies the process, saves preparation time, and reduces costs. A method for adjusting the Al content in the aerogel by changing the washing time of the sol during the ion impurity removal process is also presented. The volume stabilities and thermal properties of the Al-modified silica aerogels after high-temperature treatment are investigated. The results indicate that a small amount of modified Al improves the volumetric stability of an aerogel owing to viscous sintering of the Si–O–Al^{IV}–$(O–Al^{VI})_y$ units, which increases the disorder of the SiO_2 structure, building a barrier to viscous flow and hindering mass transfer.

Graphical Abstract

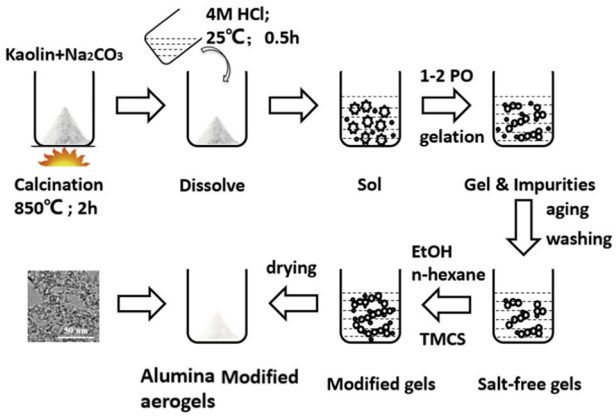

Highlights

- A novel method for preparing Al-modified silica aerogel through epoxide-assisted sol–gel route followed by ambient pressure drying with pretreated kaolin.
- The Al content in the aerogel can be controlled by the washing times. Besides, most of Al^{VI} and a small amount of Al^{IV} in the aerogel has been clarified by ^{27}Al NMR in the modified aerogel.
- The Al-modified aerogel improves the thermal stability of the aerogel especially in the pore structure.

✉ Wei Chen
chen.wei@whut.edu.cn

[1] State Key Laboratory of Silicate Materials for Architectures, Wuhan University of Technology, 430070 Wuhan, China

[2] School of Material Science and Engineering, Wuhan University of Technology, 430070 Wuhan, China

[3] National Engineering Laboratory for Fiber Optic Sensing Technology, Wuhan University of Technology, 430070 Wuhan, China

Keywords Epoxide-assisted gelation · Al-modified · Pore-structure stability · Ambient pressure drying

1 Introduction

Silica aerogel is a typical nano-mesoporous material with a continuous network structure that has high porosity, low density, and high specific surface area (SSA) [1–3]. The unique spatial network structure of silica aerogel hinders heat transfer, resulting in its low thermal conductivity of 0.02 W/mK [4]. However, silica aerogel suffers from inadequate thermal stability above 400 °C. The structure of silica aerogel is seriously damaged at high temperatures owing to the deterioration of pore structure [5, 6]. The shrinkage is generally divided into two steps according to heat-treatment temperature and chemical changes [7]: dehydration of Si–OH···OH–Si groups and silanol condensation occur at 200–550 °C, leading to shrinkage, whereas viscous sintering in the silica network starts at temperatures above 600 °C and causes pore collapse and further decrease in the surface area.

A two-step method is generally used to prepare Al-modified silica aerogel [8]. The common starting materials for preparing silica sol are Si alkoxides such as tetramethoxysilane and tetraethoxysilane, methyltrimethoxysilane, methyltriethoxysilane, and aqueous solutions of sodium silicate (water glass) [8–12]. Organic Al salts, such as Al alkoxides and acetates, and inorganic Al salts, such as Al nitrates and chlorides, can also be used for preparing Al sols [13, 14].

The materials used for preparing Al-modified silica aerogel are normally expensive and the two-step method adds to the complexity of the production process. Therefore, the use of alternative materials and simplification of the synthesis of Al-modified silica aerogels are desirable. The oxide components of kaolin are mainly SiO_2 and Al_2O_3 with small amounts of Fe_2O_3, TiO_2, and CaO. Kaolin is widely used in papermaking, ceramics, building, engineering, and refractory materials [15]. Kaolin can be transformed into highly reactive $NaAlSiO_4$ compounds if mixed with sodium carbonate and calcined at high temperatures [16]. The high Si and Al contents and high reactivity of $NaAlSiO_4$ compounds make it an ideal starting material for preparing Al-modified silica aerogel.

A method for preparing hydrophobic silica aerogel with kaolin as the starting material and drying at ambient pressure has been previously reported [17]. The reported process for preparing the aerogel consists of three steps: kaolin activation, preparation of wet silica gel, and hydrophobic modification. Metallic elements in the sol other than Si (mainly Al) are removed with cation-exchange resins during the preparation of the wet silica gel, which is time consuming and costly. The resultant silica aerogel contains less than 1% Al.

Considerable research effort has been dedicated to improve the thermal stability of silica aerogels. Al atoms in the silica network can enhance the pore-structure stability of silica aerogels and reduce the decrease of the surface area and pore volume by shielding adjacent Si–O···OH–Si groups and thus possibly obstructing silanol condensation [7]. A study of nanocomposite aerogels reveals that the use of Al as a second phase prevents the densification of these aerogels at 1000 °C [18]. It has also been reported that the addition of γ-Al_2O_3 reduces the sintering shrinkage of aerogel networks, and that a 6% loading of γ-Al_2O_3 powder reduces the shrinkage at 1000 °C to ~33% that of the network without the additive [19]. However, as discussed above, the incorporation of Al in silica aerogel can enhance its thermal stability. Thus, the preparation of Al-modified silica aerogel with kaolin can be simplified by skipping the removal of Al, yielding an aerogel with improved thermal stability.

Modified Al of silica aerogels has been proposed as an effective method to improve its thermal stability. Nuclear magnetic resonance (NMR) analysis has shown that Al atoms are incorporated into silica networks in both octahedral and tetrahedral sites [20]. Tetrahedral Al atoms are bonded with $Si–O_4$ tetrahedra through oxygen bridging to form networks, while the octahedral Al atoms are network modifiers and compensate the negative charge of the tetrahedral Al atoms. Homogeneous Al-modified silica aerogels can be described by a random silica network model with largely linear $(Si–O)_x$ polymers cross-linked with small $(Al–O)_y$ clusters involving $(Al^{IV}–O)$ and $(Al^{VI}–O)$ atoms [21]. Hence, the octahedrally coordinated Al atoms are generally incorporated at the end of the polymer chains, while the tetrahedrally coordinated atoms are mainly located inside the polymeric network, forming a fractal structure.

In the present study, a novel method to prepare Al-modified silica aerogel with kaolin as the starting material is developed. Sols comprising silica and Al are prepared from pretreated kaolin using an in situ reaction method. The pretreatment of kaolin simplifies the process, shortens preparation time, and reduces costs. A method for adjusting the Al content of the aerogel by changing the washing time in the ion impurity removal process is also proposed. The volumetric stability and thermal properties of the Al-modified silica aerogel after high-temperature treatment are investigated, providing invaluable information for its further application in the field of thermal insulation and fire safety.

2 Experiment

2.1 Material and preparation procedure

Kaolin clay from Maoming, China, was dried at 60 °C and then ground until it passed through a 150-μm sieve. The oxide composition of kaolin as received is given in Table 1. Besides the XRD pattern of raw material as received is given in Fig. 1. Sodium carbonate (Na_2CO_3, Sinopharm, AR grade), 1,2-PO (Sinopharm, AR grade), HCl (AR grade), ethyl alcohol (AR grade), n-hexane (AR grade), trimethylchlorosilane (TMCS, AR grade), and deionized water were used during the synthesis and treatment of the aerogels.

The preparation process is divided into five major steps, i.e., pretreatment of kaolin, preparation of sols, gelation, Al-content adjustment, and aerogel drying. The preparation of Al-modified silica aerogels with kaolin as the starting material is summarized in Fig. 2.

A mixture of kaolin (10 g) and 6 g of sodium carbonate was calcined at 850 °C in a muffle furnace for 2 h. The chemical reaction of kaolinite having the ideal chemical composition of $Al_2Si_2O_5(OH)_4$ with Na_2CO_3 is as follows:

$$Al_2Si_2O_5(OH)_4+Na_2CO_3 \rightarrow 2NaAlSiO_4+2H_2O+CO_2. \quad (1)$$

Table 1 Oxide composition of kaolin and calcined product

Sample	Oxide composition (mass%)				
	SiO_2	Al_2O_3	Na_2O	K_2O	LOI[a]
Kaolin	49.83	33.60	0.48	0.50	13.55
Calcined	46.34	31.25	21.20	0.50	0

[a]Loss on ignition at 1000 °C

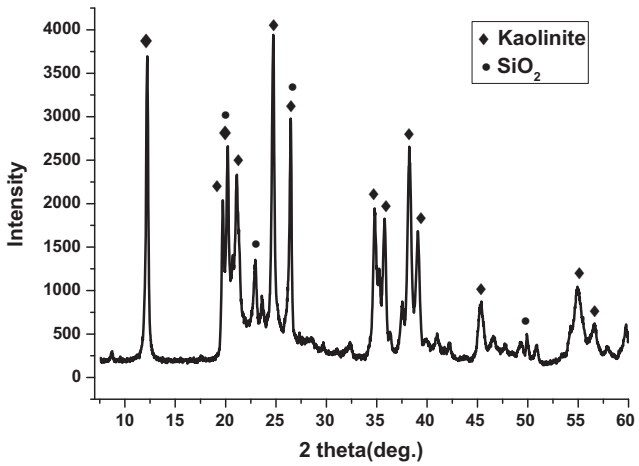

Fig. 1 Schematic illustration of the process for preparing Al-modified silica aerogels

The calcined product was cooled to room temperature and grinded to pass through a 150-μm sieve. The oxide compositions of kaolin and the calcined product are shown in Table 1, respectively.

Then, 10 g of the calcined product was dissolved in 67.5 mL of 4 M hydrochloric acid in a suit beaker. The dissolution process was accelerated by magnetic stirring for 30 min. The suspension was filtered, and the pH value of the filtrate was 2–3. The obtained silica–Al sol solution was yellow (Fig. 3). The dissolution process and the hydrolysis of the metal ions occur as follows [17, 22, 23]:

$$NaAlSiO_4+4HCl \rightarrow H_4SiO_4+AlCl_3+NaCl \quad (2)$$

$$Na_2SiO_3+2HCl \rightarrow H_2SiO_3+2NaCl \quad (3)$$

$$Al^{3+}+6H_2O \rightarrow \left[Al(H_2O)_6\right]^{3+}. \quad (4)$$

Different amounts of 1,2-PO (0–10%, v/v) were added to the yellow sols for getting an optimized amount during the epoxide-assisted gelation. Propylene oxide (1,2-PO) is added and increases the pH of the solution by absorbing the hydrogen ions. Figure 4 shows a schematic illustrating the formation of metal hydroxide from metal salt and epoxide which then undergoes polycondensation to yield polymeric or cluster-like polyoxometallates [24]. This process involves the protonation of the epoxide oxygen followed by the opening of the epoxide ring through nucleophilic attack by the conjugate base [24–26]. The relatively slow and uniform increase in the reaction pH allows controlled olation and oxolation reactions that lead to the formation of a stable metal oxide sol and a gel network is obtained. The high concentration of PO makes sure the complete reaction and accelerates the gelation. The excess PO would not make a detrimental effect for the aerogel because of the exchange of solvent during the wet gel. The network polymerization reactions are given in Eqs. (5)–(9) and $[Al(OH)_n(H_2O)_{(6-n)}]^{(3-n)}$ is formed.

$$n\left[Al(H_2O)_6\right]^{3+} \rightarrow \left[Al(OH)_n(H_2O)_{6-n}\right]^{(3-n)+}+nH^+ \quad (5)$$

$$H_4SiO_4 \rightarrow H_2SiO_3+H_2O \quad (6)$$

$$mH_2SiO_3+H_2O \rightarrow mSiO_2 \cdot (m+1)H_2O \quad (7)$$

$$2\left[Al(OH)_n(H_2O)_{6-n}\right]^{(3-n)+} \rightarrow \left[(H_2O)_{6-n}(OH)_{n-1}Al-O-Al(OH)_{n-1}(H_2O)_{6-n}\right]^{2(3-n)+}+H_2O \quad (8)$$

$$-Si-OH+\left[Al(OH)_n(H_2O)_{6-n}\right]^{(3-n)+} \rightarrow \left[Si-O-Al(OH)_{n-1}(H_2O)_{6-n}\right]^{(3-n)+}+H_2O. \quad (9)$$

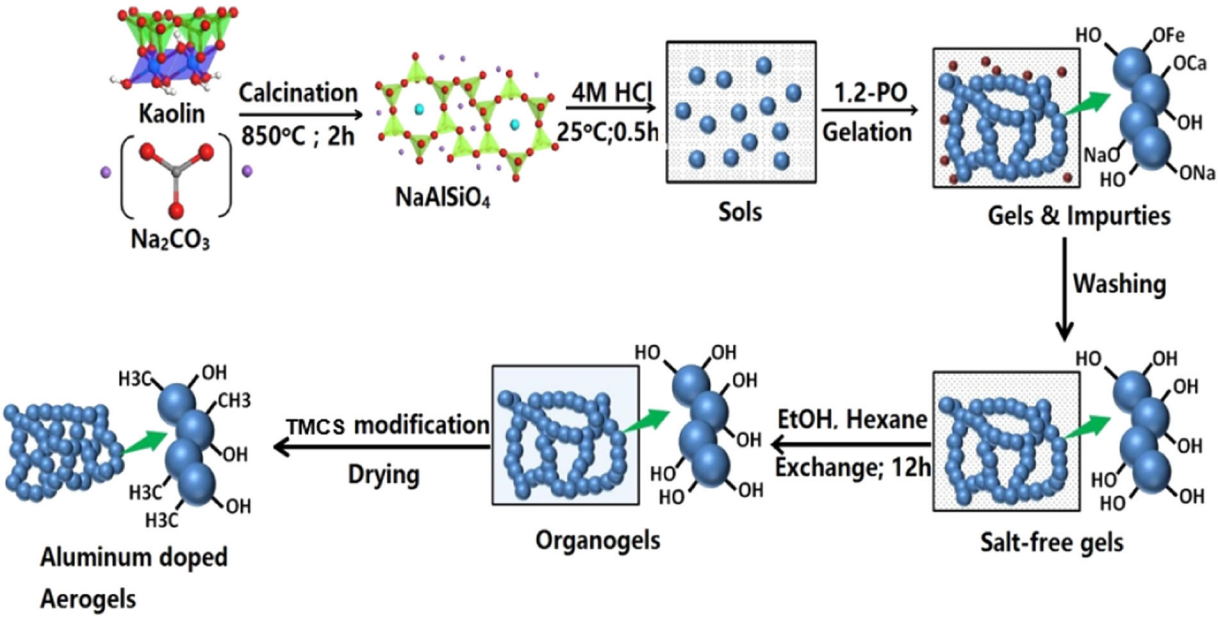

Fig. 2 Color variation of Si–Al sol transformed into Si–Al gel. **a** Si–Al sol and **b** Si–Al gel after five times washing

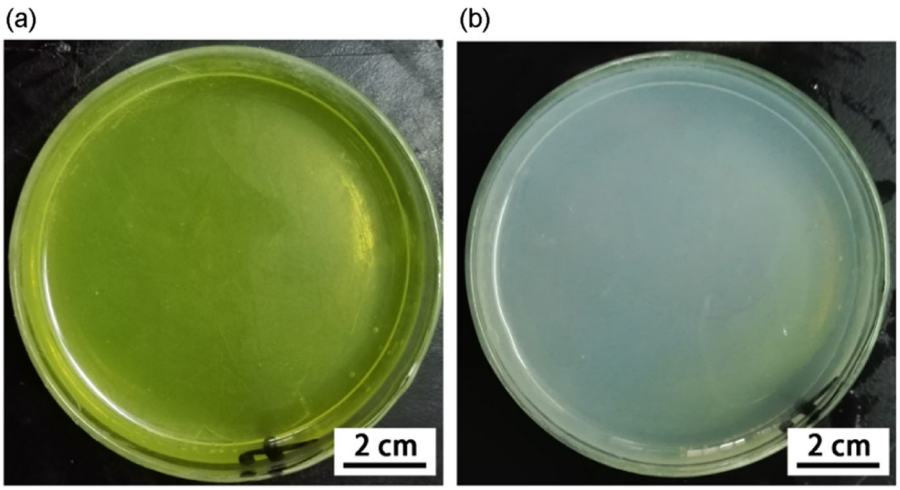

Fig. 3 Protonation and ring opening of 1,2-PO in the presence of HCl [24]

Gels formed after 5–1000 min. The obtained wet gel was aged for 24 h at 50 °C to enhance the gel network skeleton. After the aging process, the wet gel was washed by soaking with deionized water. Sodium and other impurity ions (mostly Na^+, Fe^{3+}, and Ca^{2+}) were removed by this progress, resulting in translucent gels (Fig. 3).

After washing, the aqueous gel was immersed in ethyl alcohol solution for 24 h to exchange the water inside the wet gel. This was followed by immersing the gel in n-hexane for 12 h. The surface of the wet gel was further modified by immersing it in the TMCS and n-hexane solution with an n-hexane to TMCS ratio of 1.5 by volume. The surface-modification process was considered to have completed when the gel completely floated on top of the solution. The liquid was then removed with a syringe and the remaining modified gel was washed with n-hexane.

The modified gels were dried under ambient pressure at 60 °C for 2 h, then 100 °C for 2 h, and finally 120 °C for another 2 h, after which the Al-modified silica aerogel is obtained.

2.2 Analytical techniques

The oxide compositions of the aerogels were analyzed with X-ray fluorescence spectrometry (XRF). The X-ray diffraction (XRD) patterns of the aerogels were obtained using

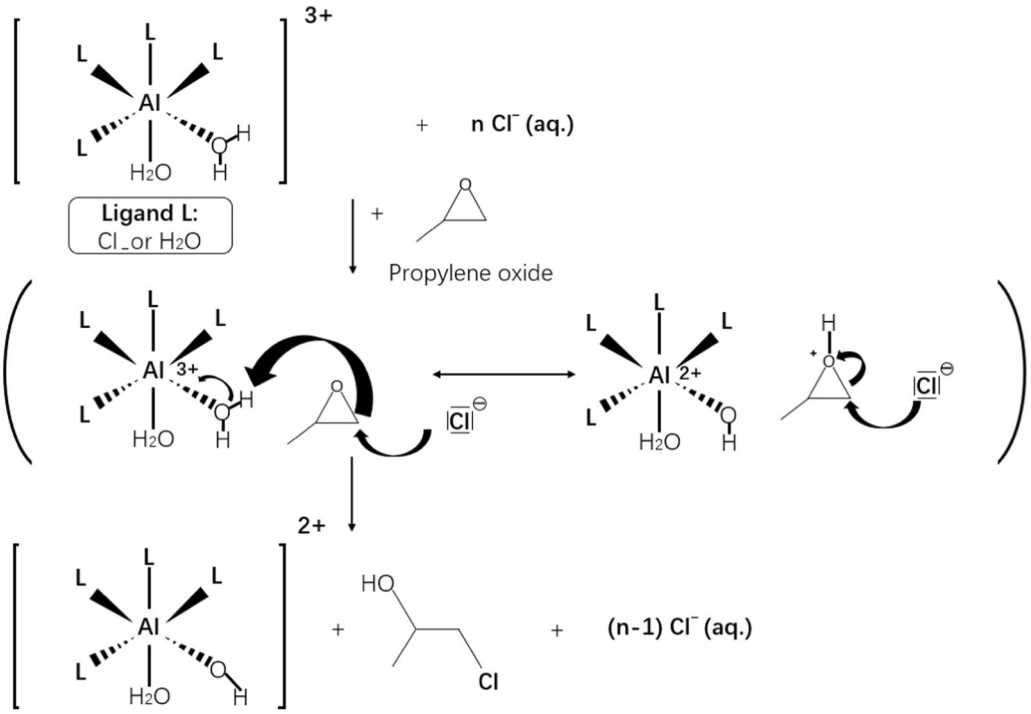

Fig. 4 XRD pattern of raw material—Maoming kaolin

Bruker D8 Advance diffractometer with Cu Kα radiation (1.5406 Å). The morphology of the aerogels after heat treatment was characterized by ULTRA PLUS-43-13 scanning electron microscope (SEM). Fourier-transform infrared (FTIR) spectra were obtained using a Thermo Nicolet Nexus FTIR spectrometer in attenuated total reflectance mode in the wavenumber range 4000–400 at 4 cm^{-1} resolution. JEM2100F transmission electron microscope was employed to observe the microstructure of aerogels and pores. The aerogel samples were dispersed in ethanol with an ultrasonic bath. A drop of the suspension was deposited on a TEM holder and dried at 80 °C for 1 h, after which the TEM image was obtained. The effective thermal conductivities of the aerogels were tested using a Hot Disk TPS2500S in transient surveying model. The aerogel powder was loaded into two cylindrical molds with 4 cm in diameter and 4-cm height. The probe was placed between the two cylindrical molds like a hamburger.

Nitrogen gas adsorption–desorption method was performed with Micromeritics Instrument Corp ASAP2020M to measure the SSAs, pore volumes, and pore sizes of the aerogels. The silica-aerogel samples were dried at 90 °C for 2 h, and then adsorption–desorption isotherms were obtained at −196.15 °C. The SSAs were calculated by using the Brunauer–Emmett–Teller theory at P/P0 <0.3 [2]. The thermal behaviors and the mass losses of the aerogels were analyzed by thermogravimetry and differential scanning calorimetry (TG-DSC) using a simultaneous thermal analyzer (Model STA449F3) in the atmosphere in the temperature range 0–1000 °C and with a heating rate of 2 °C/min.

Solid-state magic-angle spinning (MAS) ^{27}Al NMR spectra were obtained with a Bruker Avance III HD 400-MHz spectrometer using a 4-mm probe at spinning speed of 12 kHz. $Al(NO_3)_3{\cdot}9H_2O$ was used as the reference material. In order to use information found in quantitative spectra, the spectra have to be analyzed: signal areas are measured using integration, and the resulting values are used to determine concentration ratios.

The apparent densities of the aerogels were measured with a volumetric cylinder. The cylinder filled with aerogel was jolted 500 times to compact the aerogel. The apparent densities of the aerogels were calculated with Eq. (10).

$$\rho = M/V, \tag{10}$$

where ρ is the density, M is the weight, and V is the volume of the Al-modified silica aerogel, respectively. The measurements were repeated three times, and the average value of the three tests was taken as the final density of the aerogel.

Samples were heated at 200, 400, 600, and 800 °C for 2 h in a muffle furnace to characterize the stabilities and thermal conductivities of the Al-modified silica aerogels prepared using our one-step method. After calcination, the aerogels were cooled to room temperature in sealed desiccators. The volumetric change of the aerogels upon calcination was

calculated with Eq. (11).

$$\Delta V=((V_2 - V_1)/V_1)\times 100\%, \quad (11)$$

where V_1 is the volume of the aerogel before calcining, V_2 is the volume of the aerogel after calcining, and the volume change of the aerogel is denoted as ΔV. These experiments were also repeated three times, and the average value of the three test results was taken as the final volume change of the aerogel.

3 Results and discussion

3.1 Effect of 1,2-PO on gelation time

As a proton-capture agent, 1,2-PO slowly absorbs hydrogen ions through the epoxide ring-opening reaction, and a slow and uniform increase in the pH of the liquid solution is observed. The metal ions, such as $Al(OH)_4^-$, undergo a condensation reaction and form atomic clusters, which enhances the polymerization process. Polymerization products of silica and Al elements are formed and the gel skeleton is enhanced. Thus, the amount of 1,2-PO used has significant influence on the gel formation time and the microstructure of the final product aerogels.

The relationship between gelling time and 1,2-PO dosage is shown in Fig. 5. The polymerization reaction without adding 1,2-PO involves silicate alone in the solution. The pH of sol solution (2–3) made the Si–OH groups spend longer time having the polymerization reaction, resulting in a longer gelation time (~960 min). When 3% (v/v) of 1,2-PO is added, the gelation time is shortened to ~180 min, during which time the ions are fully hydrolyzed and the sol–gel transition process is easy to control, allowing the formation of a well-organized gel framework. However, if the dosage of 1,2-PO is further increased to 5 or 7% at room temperature, the gelling time is shortened to less than 20 min, indicating that the sol–gel transition process completes rapidly. Large pores that weaken the skeleton are formed owing to the rapidity of the gelation, making it more likely to be destroyed in the subsequent modification and drying processes. Thus, the dosage of 1,2-PO used in this study is 3% (v/v). The obtained wet gel was aged for 24 h at 50 °C to enhance the gel skeleton.

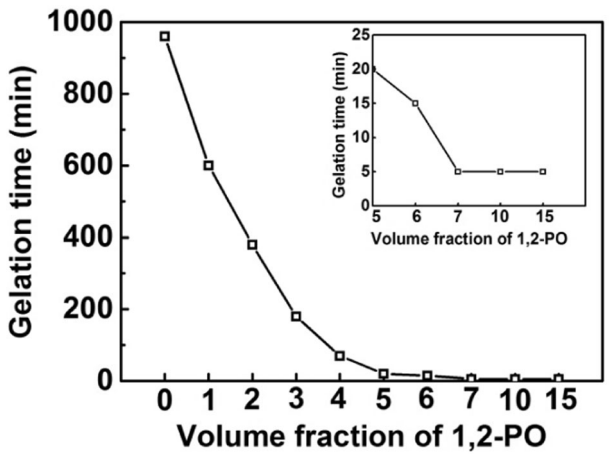

Fig. 5 Relationship between gelation time and dosages of 1,2-PO

3.2 Adjusting the aerogel Al content during the impurity removal process

Impurity removal is an indispensable step in the preparation of aerogels with kaolin owing to the presence of elements other than Al and Si. In this study, washing the gel with deionized water was used to remove the impurity cations instead of using a cation-exchange resin, as reported in other literature [17].

The factors affecting the Al contents of the aerogels are divided into internal and external factors. The internal factors are the chemical state and bonding force between the gel structures, which are directly determined by gelation and aging time. The external factors are mainly influenced by washing times. In this study, the aging time was set to 24 h in the preparation process. The Al content was adjusted by changing the washing times.

The Al contents of the modified silica aerogels after different washing times, as obtained with XRF are shown in Table 2. The Al content of the final aerogel can be up to 7.46% by mass. The amount of Al in the aerogel decreases with increasing washing times. In the washing process, the Al in the gel is dissolved into deionized water. The more times the gel is washed, the more Al will be removed from the gel. The Al content in the aerogel stabilizes at ~1.08% by mass after being washed seven times, indicating that this amount of Al is bound in the network structure of the aerogel and is difficult to remove.

The other impurity ions are alkali metal ions, which are mainly in the form of cations in the gel pore solution. With increasing washing time, the internal impurity ions leach to the deionized water, reducing the content of impurity ions in the gel. The mass fraction of Si increases with increasing washing time. This is because most of the Si is present in

Table 2 Oxide composition of Al-modified silica aerogels after different washing times (mass%)

Washing times	Al_2O_3	SiO_2	LOI[a]	Other elements
1	10.73	52.33	18.74	18.22
3	7.46	68.41	16.75	7.38
5	5.35	79.64	11.71	3.30
7	1.08	81.91	14.74	2.27

[a]Loss on ignition at 1000 °C

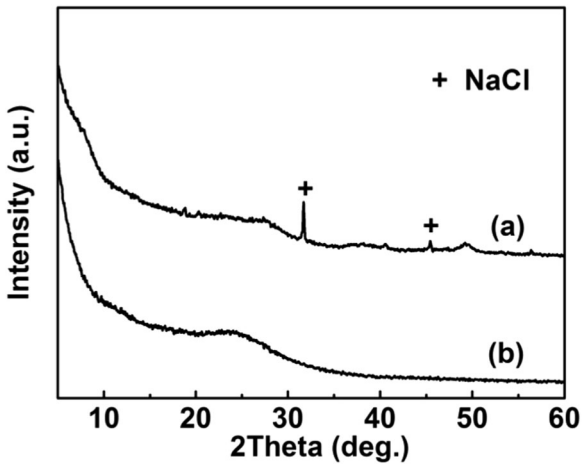

Fig. 6 XRD patterns of Al-modified silica aerogels **a** with 7.46% aluminum after three times washing and **b** with 5.35% aluminum after five times washing

the polymer network and thus very little Si is leached, even with extended washing times.

The XRD patterns of Al-modified silica aerogels with different Al contents are shown in Fig. 6. The characteristic peaks of NaCl are observed in the aerogel with 7.46% Al prepared with three washes, indicating the presence of residual Na ions and a small amount of other alkali metal ions (K). The presence of alkali metal ions weakens the aerogel frameworks and results in densification of the aerogels. No obvious crystalline phase is identified in the aerogel with 5.35% Al prepared with five washes, which suggests that most impurity ions are removed with five washes.

3.3 Structural characterization of Al-modified SiO_2 aerogels

The nitrogen adsorption–desorption isotherms of Al-modified silica aerogels with different Al contents are shown in Fig. 7. All the isotherms are type IV, which is characteristic of mesoporous materials according to IUPAC

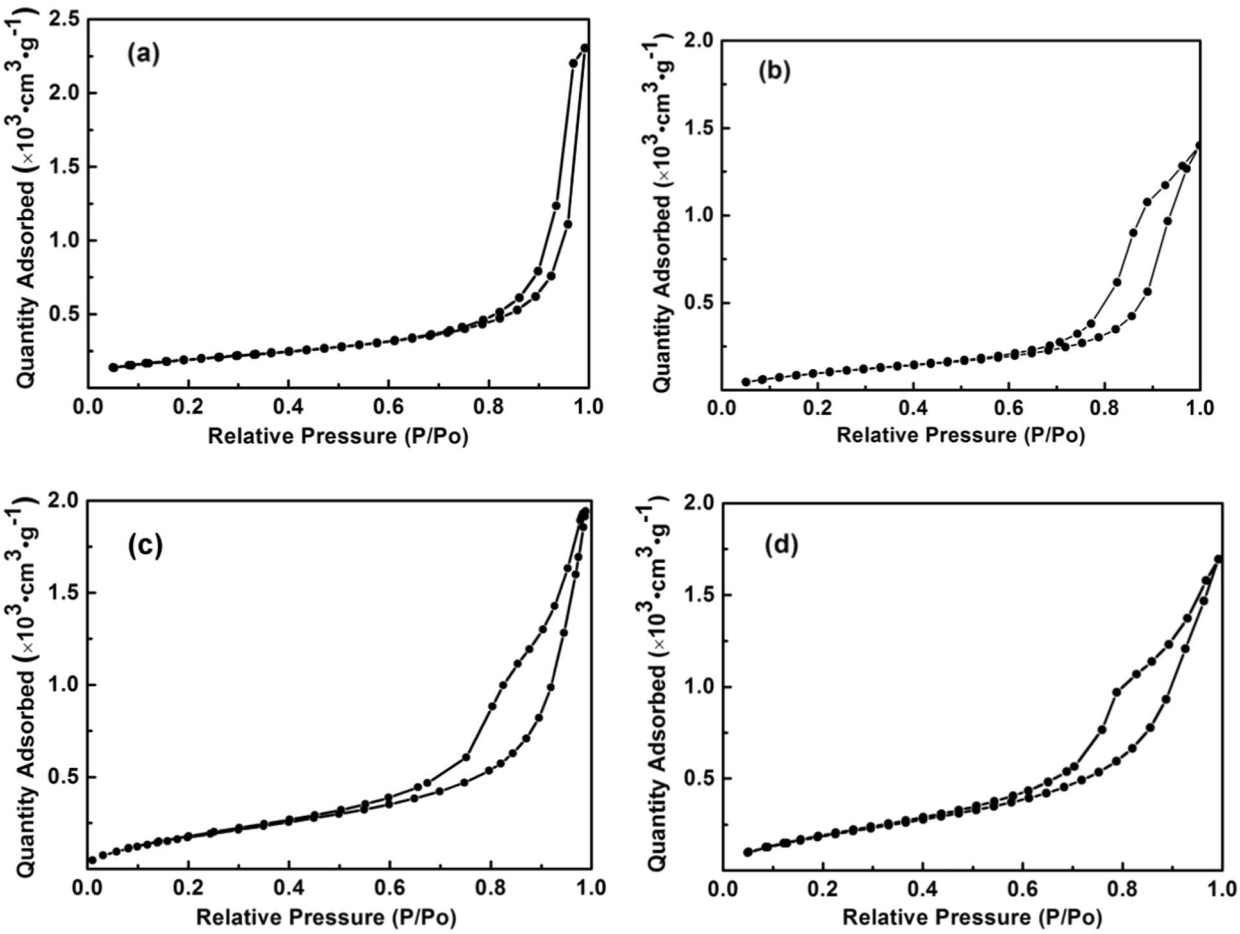

Fig. 7 Nitrogen adsorption–desorption isotherms of Al-modified silica aerogels with different aluminum content by mass. **a** 10.73%, **b** 7.46%, **c** 5.35%, and **d** 1.08%

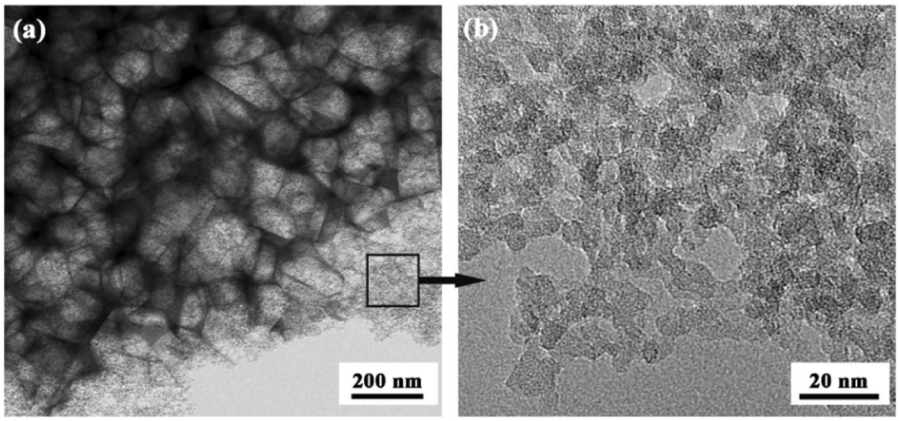

Fig. 8 **a** TEM images of SiO_2 aerogel modified with 5.35% aluminum. **b** Enlargement images of the area marked with a black arrow

classification. The hysteresis loop is type H1 according to the IUPAC classification, which is characteristic of cylindrical pores [27].

The SSAs of the Al-modified SiO_2 aerogels prepared in this study (between 439 and 492 m^2/g) are close to those of SiO_2–Al_2O_3 aerogels reported in the literature (253–729 m^2/g) [11], for which Al tri-sec-butoxide and tetraethyl orthosilicate were used as the starting materials.

The microstructure of the SiO_2 aerogel modified with 5.35% Al was observed using TEM (Fig. 8). The aerogel clearly has a three-dimensional network structure with nanosized pores in the skeleton. The aerogel particles are connected with each other and some particles are agglomerated.

The FTIR spectra and chemical bond analysis of an aerogel modified with 5.35% Al are shown in Fig. 9. The absorption peaks at 1093 and 468 cm^{-1} correspond to Si–O–Si vibrations [28]. The absorption peaks at 3423 and 1634 cm^{-1} correspond to hydroxyl groups from both physically absorbed and chemically bound water [29]. The absorption peak at 802 cm^{-1} corresponds to vibrations of Al–O bonds. Furthermore, the absorption peak at 713 cm^{-1} corresponds to Si–O–Al vibrations [30], indicating the incorporation of Al and confirming the bonding of Al with Si–O species. The absorption peaks at 2925, 2521, and 1424 cm^{-1} correspond to C–H bonds, indicating that $–CH_3$ groups are attached to the surfaces of the aerogels. The presence of these organic groups can decrease the surface tension of a gel and reduce contraction caused by excessive surface tension during the drying process.

The ^{27}Al MAS NMR spectrum for the aerogel modified with 5.35% Al is shown in Fig. 10. Quadrupolar interactions lead to the diorder of the Al NMR peaks. The three peaks around 0, 38, and 64 ppm show the presence of hexacoordinated, pentacoordinated, and tetracoordinated Al, respectively. These results indicate that most of the Al atoms in the gel are six-coordinated (Al^{VI}) as network modifiers, with fewer four-coordinated Al atoms (Al^{IV}) as

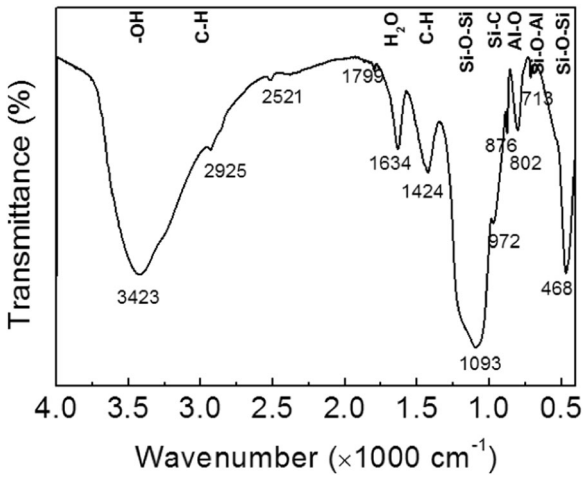

Fig. 9 FTIR spectra of silica aerogels modified with 5.35% aluminum

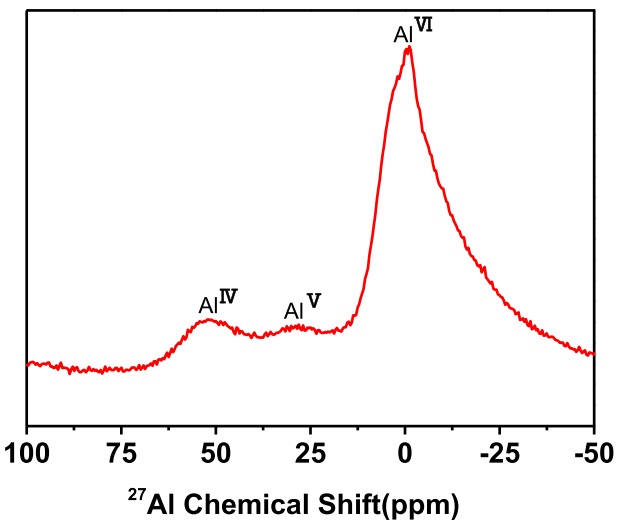

Fig. 10 ^{27}Al NMR spectrum of silica aerogels modified with 5.35% aluminum

network formers. The presence of a minor amount of pentacoordinated Al (Al^{V}) is also observed, showing that some four-coordinated Al atoms are in a distorted environment. The ratio of Al atoms in different chemical environments to total Al atoms, obtained by integrating the signal from the ^{27}Al MAS NMR spectrum is listed in Table 3. The ratio of (Al^{IV} +Al^{V}) to Al^{VI} is 0.218, which is close to the values reported in the literature [20, 21], and indicates the bonding of $(Si–O)_x$ polymers with $O–Al^{IV}–(–Al^{VI}–O)_y$ clusters.

3.4 Thermal stability of Al-modified SiO_2 aerogels

The volume changes of Al-modified silica aerogels thermally treated at different temperatures are shown in Fig. 11. The volume changes for all the aerogel samples proceed through four stages during the heat-treatment process. When the heat-treatment temperature is below 200 °C, the aerogels show very little shrinkage, mainly comprising drying shrinkage induced by loss of physically bound water. As the temperatures increases to 400 °C, the hydrophobic aerogel with $Si–(CH_3)_3$ groups gets oxidized into Si–OH, and the aerogels show expansion.

When the heat-treatment temperature increases further to 600 °C, severe shrinkage of up to 50% is observed owing to the continuous dehydration of Si–OH···OH–Si groups and collapse of the pore structures. When the temperature is increased to 800 °C, the volume shrinkage increases drastically owing to the complete destruction of the pore structure and partial sintering of the Al-modified silica aerogel.

The effects of Al content on the thermal–volumetric performance of the aerogels are marginal in the temperature range between room temperature and 400 °C. However, the effects become more prominent when the temperature is increased to 600 °C. The volumetric shrinkage of the aerogels decreases significantly with increasing Al content. The volume shrinkage of the aerogel modified with 5.35% Al is ~20% at 600 °C and 42% at 800 °C, while that of the aerogel modified with 1.08% Al is ~30% at 600 °C and 60% at 800 °C. The Al in the aerogel shields adjacent $(Si–O)_x$–$(Al–O)_y$–$(Si–O)_x$ zones between silanol groups and provides barriers to the dehydration of Si–OH···OH–Si groups [11, 21], which is beneficial for the thermal stability of the aerogel. The rationale for the improved thermal stability of the Al-modified SiO_2 aerogels is further discussed with the TG-DSC analysis results.

The physical properties of the Al-modified silica aerogels after elevated-temperature treatment are listed in Table 4. The SSA and pore volume increase slightly at 400 °C, which is consistent with the expansion of aerogels induced by spring back. After an elevated-temperature treatment at 800 °C for 2 h, the SSA and pore volume drastically decrease, while the density increases to ~0.4 g/cm^3.

The thermal conductivities of the Al-modified silica aerogels which were pretreated at different temperatures are shown in Fig. 12. The changes of the thermal conductivity are closely related to the changes of the pore structure of the aerogel. The thermal conductivity of the aerogels with different Al contents is similar (0.030–0.039 W/mK at room temperature). When the environment temperature increases to 400 °C, the thermal conductivities of the Al-modified silica aerogels slightly decrease to 0.025–0.028 W/mK, which results from spring back and pore volume increase. The effects of Al content on the thermal conductivities of the aerogels are marginal at 400 °C. The thermal

Table 3 The quantities' analysis of ^{27}Al MAS NMR spectrum

	Al^{IV}/ Al^{total}	Al^{V}/ Al^{total}	Al^{VI}/ Al^{total}	(Al^{IV} + Al^{V})/Al^{total}
Aerogels with 5.35% Al	0.130	0.088	0.782	0.218

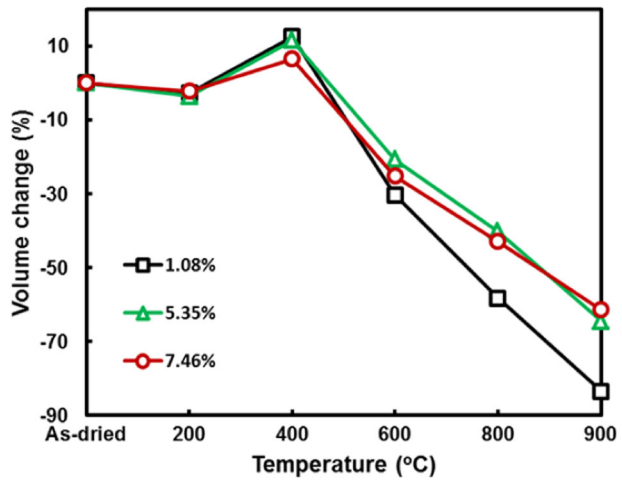

Fig. 11 Volume change of aluminum-modified SiO_2 aerogels thermally treated at different temperatures

Table 4 Physical properties of Al-modified silica aerogels after elevated-temperature treatment

Al_2O_3 content (%)	SSA (m^2/g)			Pore volume (cm^3/g)			Density (g/cm^3)		
	As-dried	400 °C	800 °C	As-dried	400 °C	800 °C	As-dried	400 °C	800 °C
1.28	492.55	709.33	136.75	2.70	2.94	0.98	0.15	0.11	0.42
5.35	455.03	571.35	128.47	2.69	2.94	1.02	0.11	0.10	0.39
7.46	439.78	489.45	198.08	2.07	2.27	1.38	0.20	0.22	0.45

conductivities of the aerogels increase significantly at 800 °C, which is due to destruction of the pore structures. Increasing Al content results in lower thermal conductivities at 800 °C. The thermal conductivities at 800 °C are 0.064 W/mK with 5.35% Al and 0.057 W/mK with 7.36% Al, while that of the aerogel modified with 1.08% Al is ~0.074 W/mK. Thus, the presence of Al in the aerogel is beneficial for lower thermal conductivities at high temperatures.

The microstructural changes of the Al-modified silica aerogel containing 5.37% Al upon elevated-temperature treatment were characterized by SEM analysis. Refined aerogel particles and homogeneous pores can be observed in Fig. 13a. More compact silica-aerogel particles and obvious pore collapse after the elevated-temperature treatment at 600 and 800 °C can be observed in Fig. 13c and d, respectively. The presence of agglomerated particles in the pores suggests partial sintering of the Al-modified silica aerogel.

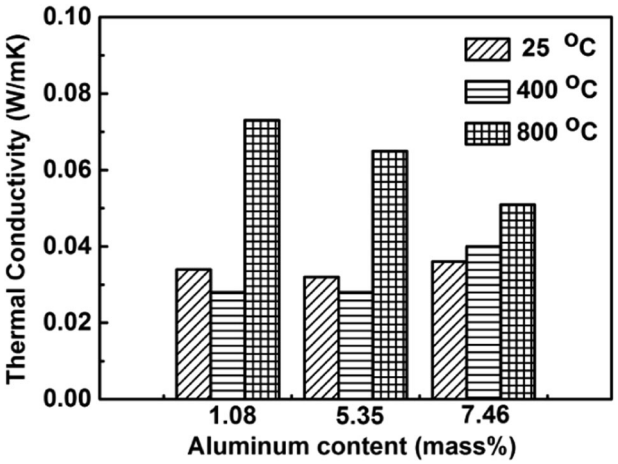

Fig. 12 Thermal conductivities of Al-modified silica aerogels at different temperatures

3.5 Thermal analysis of Al-modified silica aerogel

The Al-modified aerogels were further analyzed with TG-DSC. The results obtained with the as-dried aerogel modified at 1.08 and 5.35% Al are presented in Fig. 14. Two exothermic peaks in the DSC measurements are observed at temperatures of ~470 and 610 °C. The first exothermic peak at about 470 °C is attributed to the –Si–$(CH_3)_3$ oxidation. Dehydration of Si–OH···OH–Si groups to Si–O–Si is mainly responsible for aerogel shrinkage in the first stage. It seems that the aerogel with a lower Al content exhibits stronger resistance to condensation because its exothermic peaks appear at 504 °C (Fig. 11a) and 474 °C (Fig. 11b). However, dehydration of Si–OH···OH–Si is an endothermic reaction, while –Si–$(CH_3)_3$ oxidation is strongly exothermic. Therefore, the first exothermic peak suggests the combustion of methyl groups on the surface of the silica rather than condensation.

It is noteworthy that dehydration results in water release and significant weight loss. Besides, the oxidation of –Si–$(CH_3)_3$ to –Si–OH or –Si–O–Si slightly decreases the mass. Thus, the dehydration of Si–OH···OH–Si groups is characteristic of the DTG results. The maximum weight losses of the aerogels modified with 1.08 and 5.35% Al are

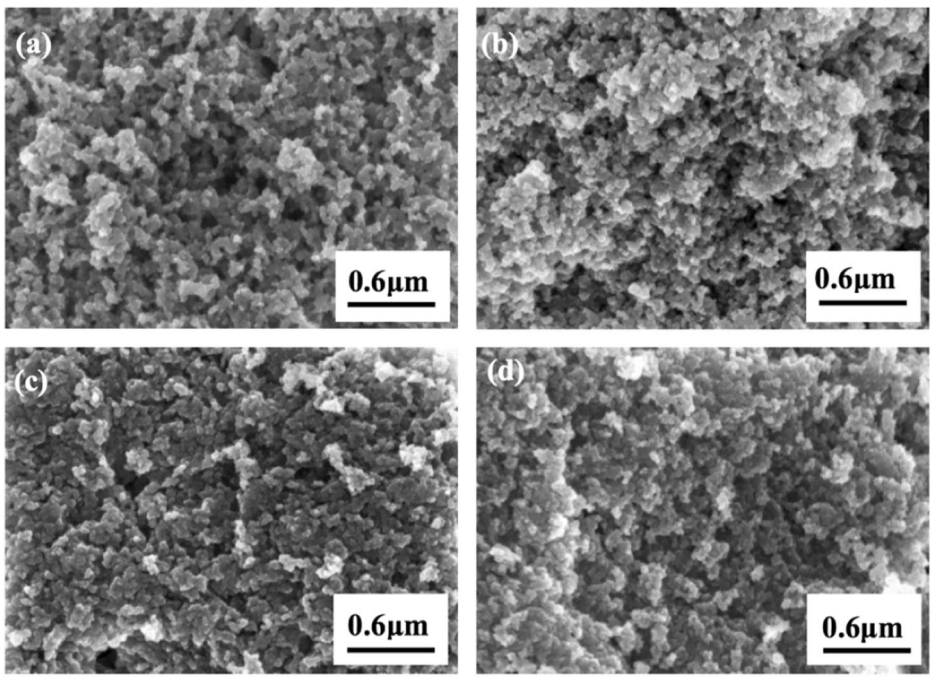

Fig. 13 Microstructural changes of Al-modified silica aerogels containing 5.37% aluminum after elevated-temperature treatment. **a** Room temperature, **b** 400 °C, **c** 600 °C, and **d** 800 °C

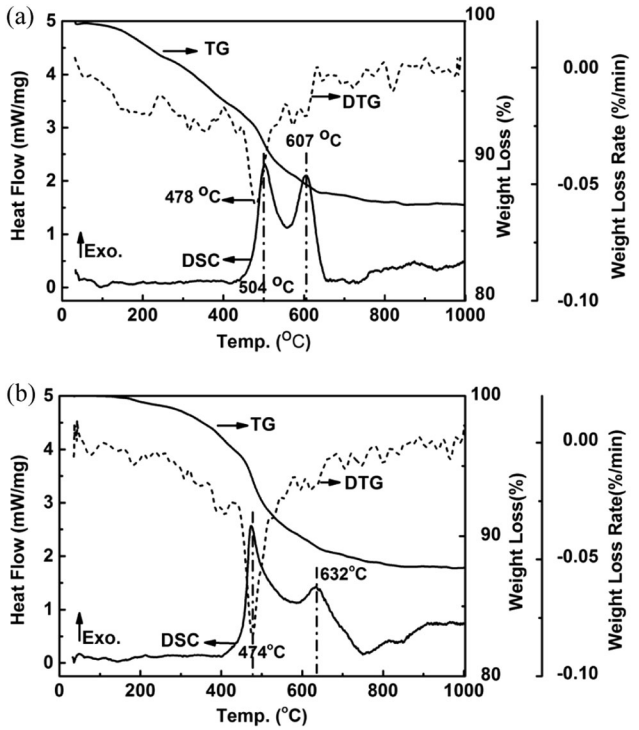

Fig. 14 TG-DSC curves of silica aerogels with different aluminum content. **a** 1.08% and **b** 5.35%

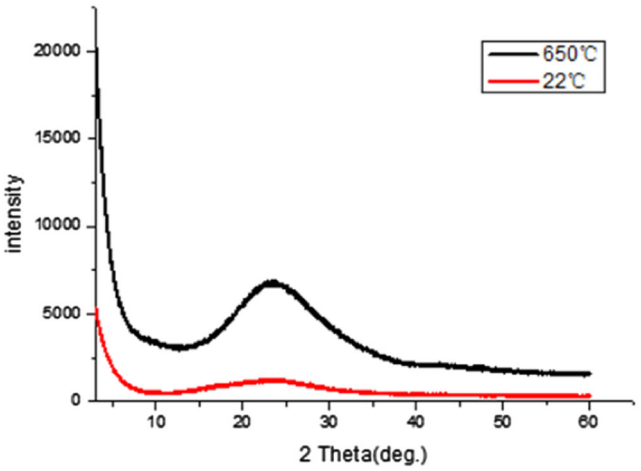

Fig. 15 XRD pattern of the aerogel at **a** 22 °C and **b** calcined at 650 °C

Table 5 Quantitative weight losses of Al-modified silica aerogels

Temperature (°C)	50–200[a]	200–400[b]	400–550[c]	550–800[d]
With 1.08% Al	1.60	3.57	5.38	2.42
With 5.35% Al	0.75	3.09	5.16	2.74

[a]Bound water

[b]Capillary solvent

[c]Oxidation of Si–$(CH_3)_3$ and condensation among silanol

[d]Viscous sintering

observed at 478 and 472 °C, respectively. The transition temperature from Si–OH···OH–Si groups to a Si–O–Si network is assumed to be ~470 °C, which indicates the similar thermal stabilities of the aerogels modified with 1.08 and 5.35% Al.

The second exothermic peak appears at 607 °C (Fig. 11a) and 632 °C (Fig. 11b), which is caused by the viscous sintering of the silica–Al skeleton and partial transition of amorphous SiO_2 to crystalline SiO_2. The XRD of the aerogel which had been calcinated at 650 °C is shown in Fig. 15. It can be concluded that the SiO_2 aerogel modified with 5.35% Al is more thermally stable than the SiO_2 aerogel modified with 1.08% Al in regard to viscous sintering. This observation shows complete consistency with the volume changes discussed in the section "Thermal stability of Al-modified SiO_2 aerogels". It has been proposed that, in the microstructure of aerogels with low Al contents (e.g., a mass percentage smaller than 10%), cross-linking between the linear $(Si–O)_x$ polymers is achieved by small $Si–O–Al^{IV}–(O–Al^{VI})_y$ units [11]. The distorted intermediate Al clusters drastically increase the disorder of the SiO_2 frameworks, which forms barriers to viscous flow and reduces mass flux in the viscous sintering process. As a result, the crystal transformation of amorphous SiO_2 and damage temperature of a silica-aerogel structure are delayed by modified Al.

The quantitative weight losses of the Al-modified silica aerogels are given in Table 5. Weight losses of 1.60 and 0.75% below 200 °C are caused by evaporation of hydroxyl-bound water. The weight losses at temperatures between 200 and 400 °C are caused by the oxidation of Si–$(CH_3)_3$. The condensation between silanol groups occurs at ~400–550 °C, resulting in water release of about 3.57 and 3.09%, respectively. The weight loss of approximately 2.5% at 550–800 °C is caused by the partial sintering of the aerogel.

4 Conclusion

Al-modified silica aerogels were produced by epoxide-assisted sol–gel route followed by ambient pressure drying with kaolin as the starting material. We established that the thermal properties of the final product were affected by the Al content in the aerogel. We investigated the effect of 1,2-PO on gelation, the adjusting of Al content, structural characterization, and thermal stability of Al-modified silica aerogel. The optimized value of 1,2-PO (3%, v/v) which was effective and economical on assisting the sol–gel procedure is demonstrated. The Al content could be controlled by changing the washing time of the wet gels soaking in the deionized water during the ion impurity removal process. And the 27Al NMR spectrum shows that most of Al^{VI} and a

small amount of Al^{IV} were present in the modified aerogel which is according to the result that most Al was water soluble in the silica aerogel and a small amount of Al was present as the network forms. The SSAs of the Al-modified silica aerogel prepared in this study varied from 439 m^2/g to 492 m^2/g, and decreased with the increase in the content of Al. Besides, the presence of Al in the aerogel is beneficial for the lower thermal conductivities at a temperature below 800 °C.

Preparing Al-modified silica aerogels with kaolin is a promising strategy owing to the low cost of the raw materials, straightforward preparation process, and make the in situ use of Al in the raw material. Further work would be focused on preparation of the pure Al-modified silica aerogel and the thermal performance above 800 °C to perfect the whole work.

Acknowledgements This research has been financially supported by the Nature Science Foundation of Hubei province (Project 2015CFA121) and Fundamental Research Funds for the Central Universities (WUT: 2017-YB-008 and 2017II010XZ).

Compliance with ethical standards

Conflict of interest The authors declare that they have no conflict ofinterest.

References

1. Gurav JL, Jung I-K, Park H-H, Kang ES, Nadargi DY (2010) Silica aerogel: synthesis and applications. J Nanomater 2010:1–11
2. Lee K-H, Kim S-Y, Yoo K-P (1995) Low-density, hydrophobic aerogels. J Non Cryst Solids 186:18–22
3. Omranpour H, Motahari S (2013) Effects of processing conditions on silica aerogel during aging: role of solvent, time and temperature. J Non Cryst Solids 379:7–11
4. Liang X (2014) The study on the preparation and performance of high performance aerogel insulation materials. University of Guangzhou, Guangzhou
5. He Y-L, Xie T (2015) Advances of thermal conductivity models of nanoscale silica aerogel insulation material. Appl Therm Eng 81:28–50
6. Amlouk A, El Mir L, Kraiem S, Alaya S (2006) Elaboration and characterization of TiO2 nanoparticles incorporated in SiO2 host matrix. J Phys Chem Solids 67(7):1464–1468
7. Aravind PR, Mukundan P, Krishna Pillai P, Warrier KGK (2006) Mesoporous silica–alumina aerogels with high thermal pore stability through hybrid sol–gel route followed by subcritical drying. Microporous Mesoporous Mater 96(1–3):14–20
8. Aegerter MA (2011) Advances in sol-gel derived materials and technologies. Springer, Berlin
9. Nadargi DY, Rao AV (2009) Methyltriethoxysilane: new precursor for synthesizing silica aerogels. J Alloy Compd 467 (1–2):397–404
10. Nadargi DY, Latthe SS, Hirashima H, Rao AV (2009) Studies on rheological properties of methyltriethoxysilane (MTES) based flexible superhydrophobic silica aerogels. Microporous Mesoporous Mater 117:617–626
11. Nadargi DY, Latthe SS, Rao AV (2009) Effect of post-treatment (gel aging) on the properties of methyltrimethoxysilane based silica aerogels prepared by two-step sol–gel process. J Sol Gel Sci Technol 49(1):53–59
12. Rao AV, Kalesh RR (2004) Organic surface modification of TEOS based silica aerogels synthesized by co-precursor and derivatization methods. J Sol Gel Sci Technol 30(3):141–147
13. Sinkó K, Hüsing N, Goerigk G, Peterlik H (2008) Nanostructure of gel-derived aluminosilicate materials. Langmuir 24(3):949–956
14. Dunphy DR, Singer S, Cook AW, Smarsly B, Doshi DA, Brinker CJ (2003) Aqueous stability of mesoporous silica films doped or grafted with aluminum oxide. Langmuir 19:10403–10408
15. Zhang ZH, Zhu HJ, Zhou CH, Wang H (2016) Geopolymer from kaolin in China: An overview. Appl Clay Sci 119(Part 1):31–41
16. Ptáček P, Šoukal F, Opravil T, Nosková M, Havlica J, Brandštetr J (2010) The kinetics of Al–Si spinel phase crystallization from calcined kaolin. J Solid State Chem 183(11):2565–2569
17. Hu W, Li M, Chen W, Zhang N, Li B, Wang M, Zhao Z (2016) Preparation of hydrophobic silica aerogel with kaolin dried at ambient pressure. Colloids Surf A Physicochem Eng Asp 501:83–91
18. Komameni S, Roy R, Selvaraj U, Malla PB, Breval E (1993) Nanocomposite aerogels: the SiO2-Al2O3 system. Mater Res Soc 8(12):3163–3167
19. Padmajaa P, Warriera KGK, Padmanabhanb M, Wunderlichc W, Berryd FJ, Mortimerd M, Creamer NJ (2006) Structural aspects and porosity features of nano-size high surface area alumina–silica mixed oxide catalyst generated through hybrid sol–gel route. Mat Chem Phys 95:56–61
20. Sinkó K (2010) Influence of chemical conditions on the nanoporous structure of silicate aerogels. Materials 3(1):704–740
21. Hernandez C, Pierre AC (2001) Evolution of the texture and structure of SiO_2–$Al2O_3$ xerogels and aerogels as a function of the Si to Al molar ratio. J Sol Gel Sci Technol 20(3):227–243
22. Wu X, Shao G, Cui S, Wang L, Shen X (2016) Synthesis of a novel Al_2O_3–SiO_2 composite aerogel with high specific surface area at elevated temperatures using inexpensive inorganic salt of aluminum. Ceram Int 42(1, Part A):874–882
23. Brahmi D, Merabet D, Belkacemi H, Mostefaoui TA, Ouakli NA (2014) Preparation of amorphous silica gel from Algerian siliceous by-product of kaolin and its physico chemical properties. Ceram Int 40(7, Part B):10499–10503
24. Koebel MM, Nadargi DY, Jimenez-Cadena G et al. (2012) Transparent, conducting ATO thin films by epoxide-initiated sol-gel chemistry: a highly versatile route to mixed-metal oxide films. ACS Appl Mater Interfaces 4(5):2464
25. Nadargi D, Kelly C, Wehrs J et al. (2014) Epoxide assisted metal oxide replication (EAMOR): a new technique for metal oxide patterning. RSC Adv 4(69):36494–36497
26. Alexander EG, Thomas MT, Joe HS et al. (2001) Use of epoxides in the sol−gel synthesis of porous iron(III) oxide monoliths from Fe(III) salts. Chem Mater 13(3):999–1007
27. P BE, G JL, P HP (1951) The determination of pore volume and area distributions in porous substances. I. Computations from nitrogen isotherms. J Am Chem Soc 73:373–380
28. Shi F, Liu J-X, Song K, Wang Z-Y (2010) Cost-effective synthesis of silica aerogels from fly ash via ambient pressure drying. J Non Cryst Solids 356:2241–2246
29. Wang L (2006) The experimental research of silica aerogel was prepared using high alumina coal ash. Ph.D. thesis, China University of Geosciences, Beijing
30. Linsha V, Peer Mohamed A, Ananthakumar S (2015) Nanoassembling of thixotropically reversible alumino-siloxane hybrid gels to hierarchically porous aerogel framework. Chem Eng J 259:313–322